

Cite this: *RSC Adv.*, 2015, 5, 89659

# Quantification of acidic sites of nanoscopic hydroxylated magnesium fluorides by FTIR and $^{15}\text{N}$ MAS NMR spectroscopy†

Felix Hemmann,<sup>ab</sup> Iker Agirrezabal-Telleria,<sup>c</sup> Christian Jaeger<sup>b</sup> and Erhard Kemnitz<sup>\*a</sup>

Lewis and Brønsted sites were quantified in a series of weak acidic hydroxylated magnesium fluorides by Fourier transform infrared spectroscopy (FTIR) and solid state nuclear magnetic resonance spectroscopy (NMR) with pyridine as probe molecule. Molar extinction coefficients, which are necessary for quantitative FTIR measurements, were calculated by an easy approach. It utilizes the fact that both signals, used for the quantification by FTIR, are caused by the same deformation vibration mode of pyridine. Comparison of quantitative FTIR experiments and quantification by NMR shows that concentrations of acidic sites determined by FTIR spectroscopy have to be interpreted with caution. Furthermore, it is shown that the transfer of molar extinction coefficients from one catalyst to another may lead to wrong results. Molar extinction coefficients and concentrations of acidic sites determined by FTIR spectroscopy are affected by grinding and probably the particle size of the sample. High temperature during FTIR experiments has further impact on the quantification results.

Received 29th July 2015  
Accepted 15th October 2015

DOI: 10.1039/c5ra15116c

[www.rsc.org/advances](http://www.rsc.org/advances)

## 1. Introduction

Metal fluorides and hydroxide fluorides are interesting acidic materials because they are able to catalyze various reactions such as dehydration reactions,<sup>1,2</sup> cyclization<sup>3</sup> or halogen exchange reactions.<sup>4</sup> Their catalytic activity is related to Lewis and Brønsted acid sites on their surfaces. For instance, the reaction mechanism of the carbohydrate dehydration reaction shows a correlation to the acidic surface properties of hydroxylated magnesium fluoride catalysts. Furthermore, the acidic properties of these samples can be altered by modifying surface OH groups with fluorosulfonic species.<sup>2</sup> Distinction and quantification of acidic sites, especially of Lewis and Brønsted sites, is therefore an important task in the characterization of acidic catalysts.

Besides various other techniques,<sup>5–11</sup> transmission Fourier transform infrared spectroscopy (FTIR) with pyridine as probe molecule is a useful method for the quantification of acidic sites.<sup>12–23</sup> This is because Lewis and Brønsted acid sites can be

distinguished, and simultaneously quantified according to the Lambert–Beer law.

The application of the Lambert–Beer law requires reliable values for molar extinction coefficients. Such coefficients have been mostly determined by comparing the pyridine adsorption at various catalysts<sup>12,14</sup> and are transferred from one catalyst to another. Thereby, it is assumed that molar extinction coefficients are intrinsic to the probe molecule. Hence, that they are independent from the type of catalyst, the acidic strength of the adsorption site and the coverage degree of the surface. Selli and Forni<sup>14</sup> list molar extinction coefficients which were determined by various authors. In contrast to the assumption that molar extinction coefficients are intrinsic to the probe molecule (pyridine), molar extinction coefficients reported by Selli and Forni<sup>14</sup> show a broad distribution and differ between 0.078 and 3.03 cm  $\mu\text{mol}^{-1}$  for Brønsted sites and between 0.269 and 3.26 cm  $\mu\text{mol}^{-1}$  for Lewis sites. Hence, the determination of molar extinction coefficients by comparing pyridine adsorption at various catalysts and transfer of molar extinction coefficients from one sample to another is doubtful and these coefficients may depend on several factors.<sup>23</sup> Selli and Forni<sup>14</sup> discuss that the distribution of molar extinction coefficients is due to different experimental conditions used for the determination of these coefficients. Hence, it would be desirable to determine molar extinction coefficients for each sample individually. Anderson and others determined molar extinction coefficients for each sample individually by using a combination of micro-gravimetry and FTIR spectroscopy.<sup>13,16–18</sup> However, this combination of FTIR and micro-gravimetry requires specialized

<sup>a</sup>Humboldt-Universität zu Berlin, Department of Chemistry, Brook – Taylor – Str. 2, D-12489 Berlin, Germany. E-mail: felix.hemmann@bam.de; erhard.kemnitz@chemie.hu-berlin.de

<sup>b</sup>BAM Federal Institute for Materials Research and Testing, Division 1, Richard Willstaetter Str. 11, D-12489 Berlin, Germany. E-mail: christian.jaeger@bam.de

<sup>c</sup>Department of Chemical and Environmental Engineering, Engineering School of the University of the Basque Country (UPV/EHU), Alameda Urquijo s/n, 48013 Bilbao, Spain. E-mail: iker.agirrezabal@ehu.es

† Electronic supplementary information (ESI) available. See DOI: 10.1039/c5ra15116c

equipment<sup>18</sup> or sample mass and IR signal areas cannot be determined simultaneously.

The present study reports on an easy method for the calculation of molar extinction coefficients of pyridine at Lewis and Brønsted sites for each sample individually. This method assumes that molar extinction coefficients for Lewis and Brønsted sites are similar in size because the signals used for the quantification of Lewis and Brønsted sites both arise from the same ring deformation mode of pyridine  $\nu_{19b}$ .

Molar extinction coefficients and concentrations of acidic sites calculated with them were determined by FTIR under various experimental conditions in a series of nanoscopic hydroxylated magnesium fluorides exhibiting both Lewis and Brønsted surface sites.<sup>24–26</sup> Furthermore, concentrations of acidic sites determined by FTIR are compared with quantitative measurements by <sup>15</sup>N MAS NMR. Pyridine was used as probe molecule in all quantification experiments to ensure that the results are comparable.

## 2. Experimental

### 2.1. Preparation of the samples

Samples were prepared under argon atmosphere using Schlenk techniques. Magnesium (Aldrich, 99.98%) (7.8 g, 325 mmol) was dissolved in 400 mL methanol (dried over Mg) at room temperature overnight. After Mg was completely dissolved, the corresponding amount of hydrofluoric acid (Mg : F ratio 1 : 2) was added at room temperature. The mixtures were vigorously stirred and reacted to form highly viscous transparent sols. Four different hydroxylated magnesium fluoride catalysts were prepared, denoted as M-40, M-57, M-71 and M-87. The number refers to the HF wt% of the hydrofluoric acid, which was added to the magnesium methoxide precursor solution. The concentration of the hydrofluoric acid was checked by titration. They were aged at room temperature overnight and dried under vacuum ( $10^{-2}$  mbar) at a heating rate of  $1\text{ K min}^{-1}$  until  $100\text{ }^{\circ}\text{C}$  and kept at this temperature for 2 h.

### 2.2. NMR experiments

Solid state NMR experiments were performed on a Bruker Avance 600 spectrometer (14.1 T). All experiments were carried out at room temperature using a 7 mm magic angle sample spinning (MAS) probe for solid state NMR experiments. Proton decoupling was carried out with a  $15^{\circ}$  two pulse phase modulation (TPPM) sequence.<sup>27</sup> Data analysis was performed with the software TopSpin 2.1 (and 3.0). DMFIT was used for line fits.<sup>28</sup> <sup>15</sup>N MAS NMR spectra were recorded using the EASY method<sup>29</sup> for removing acoustic ringing at a Larmor frequency of 60.8 MHz. <sup>15</sup>N chemical shifts ( $\delta$ ) are reported relative to  $\text{CH}_3\text{NO}_2$  with internal  $\text{NH}_4\text{Cl}$  as secondary standard ( $\delta = -341\text{ ppm}$ ).<sup>30</sup>

<sup>1</sup>H-<sup>15</sup>N CPMAS (cross-polarization with magic angle sample spinning) experiments are needed for the determination of the  $T_1$  correction factors of the time optimized <sup>15</sup>N MAS NMR spectra using the Torchia method.<sup>31</sup> Quantitative spectra are obtained with pulse repetition delay of at least one  $T_1$ . Signal

areas are corrected according to their  $T_1$  value and concentrations of acidic sites are calculated with respect to the signal area of the added  $\text{NH}_4\text{Cl}$ . Details are described elsewhere.<sup>20</sup>

For the NMR measurements, 600 mg of sample were weighted in a Schlenk flask, followed by an annealing step at  $200\text{ }^{\circ}\text{C}$  under vacuum for 2 h to remove physisorbed water. Then, excess of <sup>15</sup>N-pyridine (30  $\mu\text{L}$ ; 367  $\mu\text{mol}$ ) were added and the powder was stirred for 30 min at  $150\text{ }^{\circ}\text{C}$  to ensure homogeneous pyridine distribution. After that, the sample was evacuated for 1 h at  $150\text{ }^{\circ}\text{C}$ . Rotors for magic angle spinning (MAS) NMR experiments were carefully filled in the glovebox.

### 2.3. FTIR experiments

FTIR spectra were taken on a Nicolet iS10 FTIR spectrometer of Thermo Fisher Scientific Inc. with a dTGS (deuterated triglycine sulfate) detector. Data analysis was performed with the spectrometer software Omnic 8.1. Presented spectra are difference spectra, *i.e.*, the spectrum recorded before adsorption of pyridine was subtracted from spectra taken with pyridine adsorption.

For FTIR experiments, about 10–30 mg of a sample was grounded for one minute in a vibrating mill, if not described differently, and was pressed with a pressure of 0.5 t in a self-supporting disc (radius 0.65 mm) in air. The disc was placed in a quartz cell equipped with KBr windows. Before starting adsorption and FTIR analysis, samples were heat-treated at  $200\text{ }^{\circ}\text{C}$  in vacuum ( $10^{-5}$  to  $10^{-6}$  mbar) for 2 h. Addition of known amounts of gaseous probe molecule pyridine in the cell was possible *via* a known volume connected to the quartz cell. By filling this known volume with pyridine at known pressure, controlled by a pressure gauge, the amount of introduced pyridine could be calculated according to the ideal gas law.

After the stepwise adsorption of pyridine, samples were saturated with pyridine at a pressure of 5 mbar for 10 min and weakly adsorbed pyridine molecules were desorbed at room temperature or  $150\text{ }^{\circ}\text{C}$  in vacuum ( $10^{-5}$  to  $10^{-6}$  mbar) for 30 min.

### 2.4. X-ray diffraction (XRD)

Measurements of powder samples were performed on a Seifert RD3003TT (Freiberg, Germany) with  $\text{Cu-K}\alpha$  radiation.

### 2.5. BET experiments

Surface area measurements were performed on a Micromeritics ASAP 2020 at  $-196\text{ }^{\circ}\text{C}$  by adsorption and desorption of nitrogen. Before measurement, samples were degassed at  $100\text{ }^{\circ}\text{C}$  and  $5 \times 10^{-5}$  mbar for twelve hours. Isotherms were processed by the Brunauer–Emmett–Teller method (BET).

## 3. Theoretical background of quantitative FTIR

Adsorption of pyridine at surfaces of solid catalysts and investigation of such samples by FTIR is an important tool to distinguish and prove the presence of Lewis (LPy) and Brønsted



sites (BPy). Lewis and Brønsted sites can be identified through the signals of coordinated pyridine and protonated pyridine, pyridinium ions. Table 1 shows the wave numbers of the four vibration bands which are used for their identification.

The signals at about 1450 cm<sup>-1</sup> (LPy) and 1540 cm<sup>-1</sup> (BPy) are both due to the  $\nu_{19b}$  ring deformation mode of pyridine which is affected differently by the interactions of pyridine with the adsorption sites. Both signals are used for quantitative investigations by FTIR spectroscopy.<sup>12–18</sup>

According to the Lambert–Beer law, the concentration  $c(Y)$  [ $\mu\text{mol cm}^{-3}$ ] of an acidic site Y, *i.e.* the concentration of pyridine molecules adsorbed at such sites, can be calculated from the signal area  $A_Y$  [ $\text{cm}^{-1}$ ] of a related signal.

$$A_Y = c(Y) \times d \times \varepsilon_Y \quad (1)$$

Thereby,  $d$  [cm] is the thickness of the self-supporting disc and  $\varepsilon_Y$  [ $\text{cm} \mu\text{mol}^{-1}$ ] is the molar extinction coefficient of the pyridine signal at the acidic sites Y.

For the comparison of various catalysts, it is advantageous to compare the number of acidic sites  $n(Y)$  [ $\mu\text{mol}$ ] per catalyst mass or per surface area. The number of acidic sites  $n$  is obtained by the combination of the acidic site concentration  $c$  and the disc thickness  $d$ . This combination results in number of acidic sites per area. A signal can only be obtained in the area where the IR beam interacts with the sample. Hence, it is reasonable to include the area of the IR beam in the calculation. The area of the IR beam is constant during the whole FTIR experiment and is incorporated into the molar extinction coefficient. Accordingly, the Lambert–Beer law is modified to:

$$A_Y = n(Y) \times \varepsilon'_Y \quad (2)$$

Molar extinction coefficients are according to this equation of the dimension  $\text{cm}^{-1} \mu\text{mol}^{-1}$  and can be determined by stepwise adsorption of pyridine at the catalyst. It is assumed that molar extinction coefficients are independent from the coverage degree and do not change during the adsorption. Hence, during the stepwise adsorption of pyridine the signal areas of the signals at about 1540 cm<sup>-1</sup> and 1450 cm<sup>-1</sup> increase linearly and are further plotted *versus* the amount of introduced pyridine molecules.

The total amount of introduced pyridine  $n$  is in the first adsorption steps the sum of pyridine molecules at Lewis and Brønsted sites. In combination with eqn (2) results:

$$n = n(\text{LPy}) + n(\text{BPy}) = \frac{A_{\text{LPy}}}{\varepsilon'_{\text{LPy}}} + \frac{A_{\text{BPy}}}{\varepsilon'_{\text{BPy}}} \quad (3)$$

**Table 1** FTIR-bands [in cm<sup>-1</sup>] of adsorbed pyridine between 1700 and 1400 cm<sup>-1</sup>. LPy: pyridine coordinated at Lewis sites; BPy: pyridine protonated at Brønsted sites

Band	$\nu_{8a}$	$\nu_{8b}$	$\nu_{19a}$	$\nu_{19b}$
LPy	1600–1635	1575–1585	1490–1500	1435–1460
BPy	1630–1650	1575–1585	1490–1500	1560–1510

Derivative of eqn (3) with respect to the amount of pyridine molecules  $n$  results in:

$$1 = \frac{dA_{\text{LPy}}/dn}{\varepsilon'_{\text{LPy}}} + \frac{dA_{\text{BPy}}/dn}{\varepsilon'_{\text{BPy}}} \quad (4)$$

$dA_{\text{LPy}}/dn$  and  $dA_{\text{BPy}}/dn$  are the slopes of the signal areas *versus* the amount of introduced pyridine molecules in the first adsorption steps determined in the experiments. However, eqn (4) can only be solved if only one kind of acidic sites is present in a sample. In such a case the slope of the acidic site which does not occur is zero. Hence, one summand of eqn (4) is zero and the molar extinction coefficient of the occurring site can be determined. Otherwise, if Lewis and Brønsted sites are present, eqn (4) cannot be easily solved, as there are two unknown variables. Therefore, in samples in which LPy and BPy occur, an additional condition for  $\varepsilon'_{\text{LPy}}$  and  $\varepsilon'_{\text{BPy}}$  has to be found to solve eqn (4).

Two possibilities for the calculation of  $\varepsilon'_{\text{LPy}}$  and  $\varepsilon'_{\text{BPy}}$  have been described in the literature. One possibility is to compare the slopes  $dA_{\text{LPy}}/dn$  and  $dA_{\text{BPy}}/dn$  obtained for various catalysts. The molar extinction coefficients are then calculated from the various slopes under the assumption that the extinction coefficients are the same for each catalyst.<sup>12,14</sup> However, Selli and Forni<sup>14</sup> showed that a broad distribution of molar extinction coefficients can be found in the literature, and Rosenberg *et al.* even found different molar extinction coefficients for series of similar catalysts.<sup>16,17</sup> Therefore, it is questionable to calculate  $\varepsilon'_{\text{LPy}}$  and  $\varepsilon'_{\text{BPy}}$  by comparing various catalysts. A second possibility to determine  $\varepsilon'_{\text{LPy}}$  and  $\varepsilon'_{\text{BPy}}$  is to combine microgravimetry and FTIR spectroscopy.<sup>13,16–18</sup> However, this combination requires specialized equipment<sup>18</sup> or sample mass and IR signal areas cannot be determined simultaneously. Therefore, another approach is chosen to determine molar extinction coefficients in this study.

Both signals at about 1540 cm<sup>-1</sup> and 1450 cm<sup>-1</sup>, which are used for the quantification of acidic sites, are due to the  $\nu_{19b}$  ring deformation mode of protonated pyridine at Brønsted sites and coordinated pyridine at Lewis sites. Furthermore, molar extinction coefficients for Lewis and Brønsted sites listed by Selli and Forni<sup>14</sup> or calculated in the group of Anderson<sup>13,16,17</sup> are in the same order of magnitude, whereby in most cases the molar extinction coefficient for Lewis sites is up to three times larger than the molar extinction coefficient for Brønsted sites.

Fig. 1 shows a plot for eqn (4) of possible values for  $\varepsilon'_{\text{LPy}}$  and  $\varepsilon'_{\text{BPy}}$  with  $dA_{\text{LPy}}/dn = 1$  and  $dA_{\text{BPy}}/dn = 0.5$ . As we know that  $\varepsilon'_{\text{LPy}}$  and  $\varepsilon'_{\text{BPy}}$  have to be in the same order of size, it is further assumed that the correct pair of values for  $\varepsilon'_{\text{LPy}}$  and  $\varepsilon'_{\text{BPy}}$  is the point of eqn (4) nearest to the origin of the coordinate system.

The closest pair of values ( $\varepsilon'_{\text{LPy}}$  and  $\varepsilon'_{\text{BPy}}$ ) to the origin of the coordinate system is calculated by searching the minimal value for the sum of  $\varepsilon_{\text{LPy}}'^2$  and  $\varepsilon_{\text{BPy}}'^2$  under the conditions that eqn (4) is fulfilled and both values are positive.

Differences in the molar extinction coefficients due to the nature of the solid or the acid strength of the adsorption sites between various samples have already an influence on the slope of the signal areas measured in the stepwise adsorption of



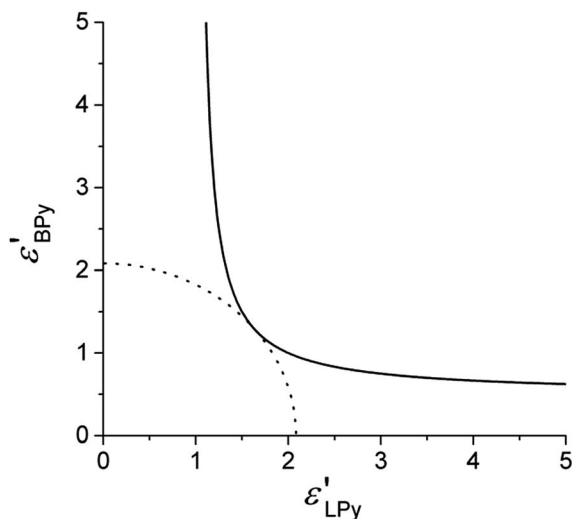


Fig. 1 Plot of eqn (4) with  $dA_{LPY}/dn = 1$  and  $dA_{BPY}/dn = 0.5$  and the corresponding function of  $\epsilon'_{LPY}{}^{1/2} + \epsilon'_{BPY}{}^{1/2}$  (dotted line).

pyridine. Hence, these factors influence eqn (4) and are therefore considered in the calculation of molar extinction coefficients.

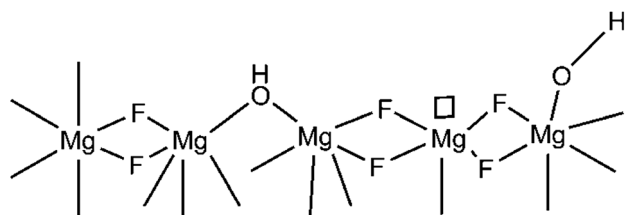
Calculated  $\epsilon'_{LPY}$  and  $\epsilon'_{BPY}$  are used to determine the amount of acidic sites. For this purpose, all acidic sites are saturated with pyridine and weakly adsorbed molecules, physisorbed pyridine or bound *via* hydrogen bridges, are desorbed from the catalyst. According to eqn (2) the amount of acidic sites can be calculated from the areas of the signals at  $1540\text{ cm}^{-1}$  or  $1450\text{ cm}^{-1}$  and their molar extinction coefficients.

$$n(Y) = A_Y/\epsilon'_Y \quad (5)$$

The concentrations of acidic sites per catalyst mass are calculated by dividing the amount of acidic sites by the mass of the investigated self-supporting disc.

## 4. Results

Hydroxylated magnesium fluorides are biacidic catalysts. Hence, besides acidic Lewis sites these catalysts also exhibit acidic Brønsted sites. The Brønsted acidic character of these catalysts is surprising because MgOH groups are usually of basic character. The partial acid character of hydroxyl groups in hydroxylated magnesium fluorides is probably caused by the



Scheme 1 Graphical illustration of the surface of a hydroxylated magnesium fluoride. The symbol (□) indicates a vacancy (Lewis) site.

mixed coordination of magnesium by fluorine and hydroxyl groups at the particle surfaces, as shown schematically in Scheme 1.<sup>24–26</sup>

Besides FTIR spectroscopy,  $^{15}\text{N}$  MAS NMR spectroscopy can be used to distinguish and quantify acidic Lewis and Brønsted sites. Hence, it was used as reference method for the quantitative FTIR experiments in the investigated series of catalysts.

The most common method for the quantification of acidic sites  $\text{NH}_3$ -TPD is not used in this study as these samples are sensitive to temperature.<sup>24</sup> As example, ESI Fig. 1† shows the X-ray pattern of a hydroxylated magnesium fluoride sample before and after it was calcinated at  $300^\circ\text{C}$ . The decrease in the peak width shows that at  $300^\circ\text{C}$  the crystallite size increase and probably some of the acidic sites are destroyed by surface rearrangement.

### 4.1. $^{15}\text{N}$ MAS NMR spectroscopy

Fig. 2 shows the  $^{15}\text{N}$  MAS NMR spectra of the four hydroxylated magnesium fluoride samples after adsorption of pyridine. The spectra show four signals. The narrow signal at  $-341\text{ ppm}$  is assigned to ammonium chloride which was added as internal standard for the quantification. The other three signals are assigned to pyridine in different adsorption states. All samples show a signal at  $-102\text{ ppm}$  with a broad sideband pattern typical for pyridine molecules coordinated at acidic Lewis sites LPy. This signal overlaps with the signal of pyridine molecules adsorbed *via* hydrogen bridges HPy at  $-89\text{ ppm}$ . A signal for protonated pyridine at Brønsted sites BPY at  $-175\text{ ppm}$  is only observed in three of the samples and not in M-40. None of the  $^{15}\text{N}$  MAS NMR spectra show a signal of bulk pyridine at about  $-64\text{ ppm}$ .<sup>32,33</sup> This means that all pyridine molecules are adsorbed at the catalyst surfaces.

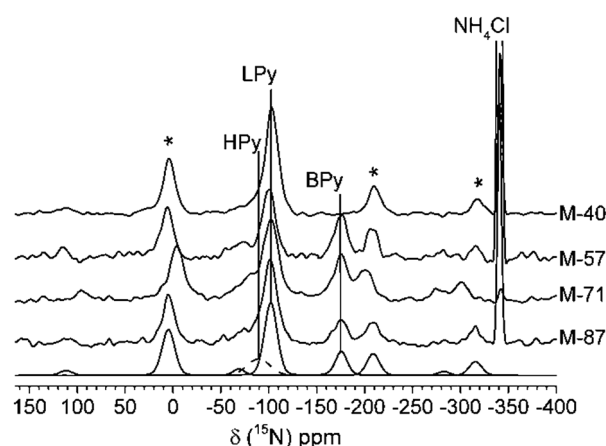


Fig. 2  $^{15}\text{N}$  MAS NMR spectra of the four hydroxylated magnesium fluorides after adsorption of pyridine. Additionally, the line fits of sample M-87 for pyridine at Lewis sites, Brønsted sites (solid lines) and pyridine molecules adsorbed *via* hydrogen bridges (dotted line) are shown. Spectra were obtained under comparable experimental conditions. MAS spinning frequency was  $6.5\text{ kHz}$  except for M-71 ( $6\text{ kHz}$ ). The signal intensity of sample M-40 is divided by two because of faster  $T_1$  relaxation. \*MAS spinning sidebands.





**Table 2** Concentrations of acidic sites determined by  $^{15}\text{N}$  MAS NMR spectroscopy for the four hydroxylated magnesium fluoride samples. The errors were determined by multiple measurements of the samples and various simulations of the spectra (NMR)

Sample	Lewis sites ( $\mu\text{mol g}^{-1}$ )	Brønsted sites ( $\mu\text{mol g}^{-1}$ )
M-40	$303 \pm 46$	—
M-57	$302 \pm 34$	$136 \pm 14$
M-71	$262 \pm 52$	$67 \pm 22$
M-87	$252 \pm 29$	$52 \pm 10$

The  $T_1$  values of all signals are determined using the Torchia method<sup>31</sup> and signal areas of signals in the  $^{15}\text{N}$  MAS NMR spectra are corrected accordingly. The concentrations of each adsorption state are determined by comparing the corrected signal areas of the individual sites with the signal area of the added internal standard ammonium chloride.<sup>3,20</sup> Concentrations of pyridine molecules adsorbed *via* hydrogen bridges were not determined as their concentrations differ depending on the sample preparation.<sup>19</sup>

Table 2 lists the concentrations of Lewis and Brønsted sites in the four samples. The concentrations of acidic Lewis sites are nearly equal in all samples, whereas the concentration of acidic Brønsted sites changes. It decreases from M-57 to M-87, while M-40 shows no Brønsted sites. The reason for the decrease in the concentration of Brønsted sites is that less hydroxyl groups are present in samples synthesized with highly concentrated hydrofluoric acid than in samples synthesized with diluted hydrofluoric acid. Hence, the number of hydroxyl groups/Brønsted sites decreases with increasing concentration of the hydrofluoric acid used for the synthesis.<sup>25</sup> The reason that M-40 shows no Brønsted sites is probably that the hydroxyl groups in this sample are too weak to protonate pyridine. It is assumed that the acid strength of

MgOH groups decrease with the increasing concentration of hydroxyl groups at the surface. Hence, hydroxyl groups at the surface of M-40 may already exhibit neutral or even basic character.

## 4.2. FTIR spectroscopy

FTIR spectroscopy can distinguish between Lewis and Brønsted sites. However, determination of molar extinction coefficients and therefore quantification of acidic sites is often challenging. As has been pointed out,<sup>14,23</sup> experimental conditions can affect the quantification by FTIR. Hence, molar extinction coefficients and concentrations of acidic sites were calculated under various sample preparation and adsorption conditions. Especially, grounding of the samples was considered because we found that ungrounded samples can be easier pressed in self-supporting discs.

**4.2.1. Ungrounded samples.** The first samples were pressed in self-supporting discs without further sample preparation, just as they were synthesized. The investigated hydroxylated magnesium fluorides are nanocrystalline what can be shown by XRD (Fig. 2 in ESI†) but can form larger agglomerates in the synthesis.<sup>34</sup>

Fig. 3 shows exemplary the stepwise adsorption spectra of pyridine on the hydroxylated magnesium fluoride sample M-57. The FTIR spectra of the stepwise pyridine adsorption on the other three samples can be found in the ESI (Fig. 3–5†). All spectra show signals for pyridine molecules coordinated at Lewis sites at about 1606, 1578, 1492, and 1445  $\text{cm}^{-1}$ . Surprisingly, only sample M-57 shows signals of pyridine molecules protonated at Brønsted sites at 1645 (very weak or not detected at all), 1578, 1545, and 1493  $\text{cm}^{-1}$  during adsorption of pyridine. Brønsted sites were also detected by  $^{15}\text{N}$  MAS NMR in sample M-75 and M-87. In these samples, the FTIR signals of pyridine molecules at Brønsted sites only appear after desorption of pyridine at 150 °C. These results suggest that Brønsted

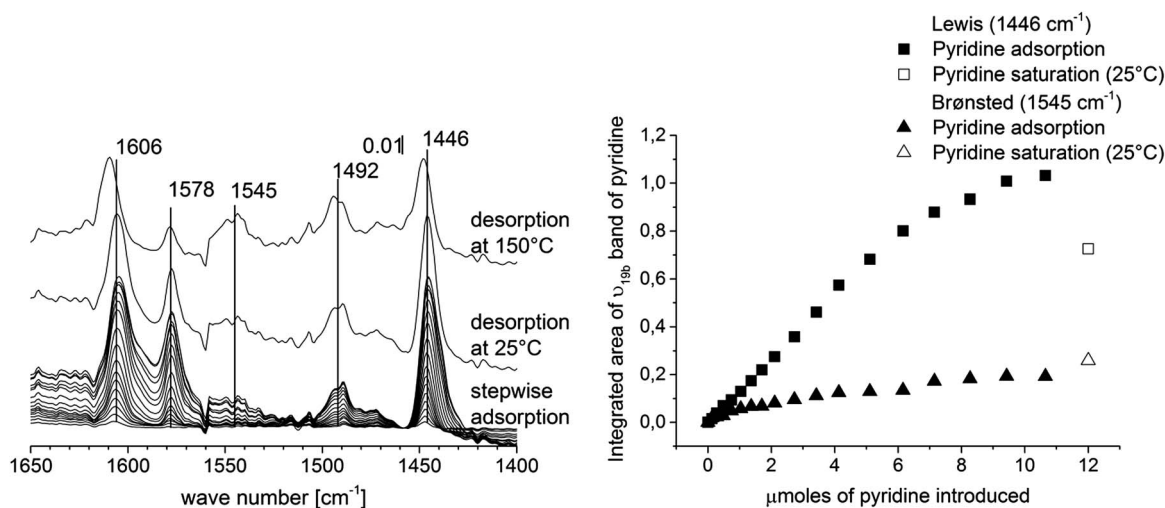


**Fig. 3** FTIR spectra after stepwise pyridine adsorption at ungrounded M-57 and the integrated intensity of  $\nu_{19b}$  band of coordinated and protonated pyridine at about 1446 and 1545  $\text{cm}^{-1}$ . Also shown are the integrated intensities of  $\nu_{19b}$  band after saturation with pyridine (open symbol).



**Table 3** Calculated molar extinction coefficients of coordinated (Lewis) and protonated pyridine molecules (Brønsted) and the concentration of Lewis and Brønsted sites in the ungrounded hydroxylated magnesium fluoride samples. Each catalyst has been investigated several times

Sample	$\epsilon'_{\text{LPy}}$ [cm <sup>-1</sup> μmol <sup>-1</sup> ]	Lewis sites [μmol g <sup>-1</sup> ]	$\epsilon'_{\text{BPy}}$ [cm <sup>-1</sup> μmol <sup>-1</sup> ]	Brønsted sites [μmol g <sup>-1</sup> ]
<b>M-40</b>				
1 <sup>st</sup>	1.19	106		
2 <sup>nd</sup>	0.35	131		
3 <sup>rd</sup>	0.30	83		
<b>M-57</b>				
1 <sup>st</sup>	0.19	105	0.12	60
2 <sup>nd</sup>	0.10	184	0.04	84
3 <sup>rd</sup>	0.19	103	0.10	63
<b>M-71</b>				
1 <sup>st</sup>	0.05	175		
2 <sup>nd</sup>	0.06	102		
3 <sup>rd</sup>	0.66	146		
<b>M-87</b>				
1 <sup>st</sup>	0.41	172		
2 <sup>nd</sup>	0.44	265		

sites are mostly inaccessible for pyridine molecules during adsorption.

Additionally, Fig. 3 (and ESI Fig. 3–5†) shows the plots of the signal areas of the signals at about 1545 and 1446 cm<sup>-1</sup> *versus* the amount of pyridine introduced. These plots show the expected behavior for the signal area of the Lewis sites *versus* introduced pyridine molecules: a first linear increase of the signal area with increasing pyridine concentration and flattening of the curve after all accessible acidic sites are saturated with pyridine. The Brønsted sites in sample M-57 are not fully saturated during the pyridine adsorption, this is an indication that the Brønsted sites are also difficult to access for pyridine in M-57 like in the other samples.

Molar extinction coefficients are calculated as described in Chapter 3 from the slopes of the signal areas *versus* the adsorbed amount of pyridine. With the molar extinction coefficients the concentrations of Lewis and Brønsted sites are calculated after all acid sites have been saturated with pyridine and weakly adsorbed pyridine has been desorbed.

Each sample was investigated up to three times by stepwise adsorption of pyridine. Table 3 lists the calculated molar extinction coefficients and determined concentrations of acidic sites. The molar extinction coefficients for Brønsted sites and concentrations of Brønsted sites were only determined for M-57 because these sites appear only after pyridine desorption at higher temperature in sample M-71 and M-87.

The molar extinction coefficients, shown in Table 3, exhibit a broad distribution. Even for the same sample, extinction coefficients differ up to a factor of 12. The concentrations of acidic sites, however, are in the same order of magnitude for each sample but show an error of up to 40% and are mostly smaller as detected by <sup>15</sup>N MAS NMR.

**4.2.2. Grounded samples.** Molar extinction coefficients and concentrations of acidic sites change if samples were finely grounded before they were pressed in self-supporting discs. Spectra of the stepwise pyridine adsorption and the plots of signal area *versus* the amount of adsorbed pyridine are shown in the ESI (Fig. 6–9†). As for the ungrounded samples, only in sample M-57 signals of Brønsted sites can be detected but the Brønsted sites are not saturated during the stepwise adsorption of pyridine.

Table 4 lists molar extinction coefficients and concentrations of acidic sites for the samples which were grounded before they were pressed in self-supporting discs. The molar extinction coefficients are bigger and show a much narrower distribution (maximum factor of 1.4 in a single sample) in the grounded samples as in the ungrounded samples. However, they still differ between the catalysts up to a factor of two.

The calculated concentrations of acidic sites also change in the grounded samples. In sample M-40, M-71 and M-87 concentrations of acidic sites are now in the same order of magnitude as determined by <sup>15</sup>N MAS NMR. Except for sample M-57, pyridine seems to reach all Lewis acidic sites during adsorption in the grounded samples. However, no Brønsted sites were detected for sample M-71 and M-87. The error of the quantification is smaller but still in the order of 30%.

**4.2.3. Adsorption at 150 °C.** Finally, pyridine was adsorbed at grounded samples at 150 °C. The FTIR spectra of the stepwise adsorption for these samples and the plotted signal areas *versus* the amount of pyridine are shown in the ESI (Fig. 10–13†). The spectra show that Brønsted sites are detected at an adsorption temperature of 150 °C in the samples M-57, M-71 and M-87.

Plots of signal areas *versus* adsorbed pyridine show in all samples the expected adsorption behavior for Lewis sites, and in sample M-57 also for Brønsted sites; the signal area increase

**Table 4** Calculated molar extinction coefficients of coordinated (Lewis) and protonated pyridine molecules (Brønsted) and the concentration of Lewis and Brønsted sites in the grounded hydroxylated magnesium fluoride samples. Each catalyst has been investigated several times

Sample	$\epsilon'_{\text{LPy}}$ [cm <sup>-1</sup> μmol <sup>-1</sup> ]	Lewis sites [μmol g <sup>-1</sup> ]	$\epsilon'_{\text{BPy}}$ [cm <sup>-1</sup> μmol <sup>-1</sup> ]	Brønsted sites [μmol g <sup>-1</sup> ]
<b>M-40</b>				
1 <sup>st</sup>	1.11	344		
2 <sup>nd</sup>	1.21	248		
3 <sup>rd</sup>	1.37	402		
<b>M-57</b>				
1 <sup>st</sup>	0.78	160	0.26	59
2 <sup>nd</sup>	0.77	96	0.28	38
3 <sup>rd</sup>	0.81	150	0.22	49
<b>M-71</b>				
1 <sup>st</sup>	1.09	378		
2 <sup>nd</sup>	1.54	218		
<b>M-87</b>				
1 <sup>st</sup>	1.01	264		
2 <sup>nd</sup>	1.44	284		



**Table 5** Calculated molar extinction coefficients of coordinated (Lewis) and protonated pyridine molecules (Brønsted) and the concentration of Lewis and Brønsted sites in the grounded hydroxylated magnesium fluoride samples at an adsorption temperature of 150 °C

Sample	$\epsilon'_{\text{LPy}}$ [cm <sup>-1</sup> μmol <sup>-1</sup> ]	Lewis sites [μmol g <sup>-1</sup> ]	$\epsilon'_{\text{BPy}}$ [cm <sup>-1</sup> μmol <sup>-1</sup> ]	Brønsted sites [μmol g <sup>-1</sup> ]
M-40	1.28	199		
M-57	0.63	72	0.45	40
M-71	1.38	154	0.50	40
M-87	0.96	251	0.32	37

linearly with increasing pyridine concentration in the beginning of adsorption and after the acidic sites are saturated the curve levels off. However, in the plot of sample M-71 and M-87, the signal areas of pyridine at Brønsted sites increase until the end of the stepwise adsorption. Again, this is an indication for the difficult accessibility of Brønsted sites in these samples.

Table 5 lists the molar extinction coefficients and concentrations of acidic sites calculated for the series of grounded samples and pyridine adsorption at 150 °C. Molar extinction coefficients for Lewis sites are in the same order of magnitude as for the grounded samples and adsorption at 25 °C. However, they still differ between the samples, especially for sample M-57. The molar extinction coefficients for Brønsted sites, in contrast, are twice as large at higher adsorption temperature.

The concentrations of acidic sites at 150 °C are smaller as calculated at 25 °C. Especially for the samples M-40, M-57 and M-71, the concentration of Lewis sites are only about half as large at 150 °C compared to the concentrations at 25 °C. The reason will be discussed in detail in the next chapters.

## 5. Discussion

Quantitative FTIR investigations by stepwise adsorption of pyridine in a series of hydroxylated magnesium fluorides show that the grinding of the samples and the temperature, at which pyridine is adsorbed have a huge impact on the calculated molar extinction coefficients and concentrations of acidic sites.

### 5.1. Comparison of molar extinction coefficients

First of all, molar extinction coefficients determined under various conditions are discussed. Molar extinction coefficients determined for grounded samples are larger in comparison to extinction coefficients of ungrounded samples. The reason may be the presence of large particles/agglomerates of hydroxylated magnesium fluoride in the ungrounded samples. Chalmers<sup>35</sup> reported that the signal intensity of an IR signal depends on the particle sizes in the sample and increases with decreasing particle size. The effect of grinding on the signal intensity becomes most visible in sample M-71. The signal intensities of the pure samples before the adsorption of pyridine (see Fig. 14 in ESI† on the left side) increase after grinding of the sample. Hence, grinding seems to lead to smaller particles/agglomerates. Surprisingly, the signal intensities of pyridine

(Fig. 14 in ESI† on the right, note that the spectra are shown in the same order as on the left side) show the same trend. Not only the signal intensities of the catalysts are affected by their particle size but also the signal intensities of pyridine adsorbed on their surface.

Molar extinction coefficients are calculated from the signal areas of the first adsorption steps and therefore are also affected by the particle sizes in the sample. Hence, molar extinction coefficients increase in the same way as the signal area of adsorbed pyridine with decreasing particle size. It has been reported very recently that particle sizes have an effect on molar extinction coefficients of adsorbed molecules.<sup>36</sup> However, Jentoft *et al.*<sup>36</sup> found that molar extinction coefficients of adsorbed alkanes increase with higher scattering of a sample, respectively larger particles. This is in contrast to the presented observations that molar extinction coefficients of pyridine increase with decreasing scattering/particle size of a sample.

Variation of sample weights can be ruled out as reason for the difference in the signal areas, respectively the molar extinction coefficients (differ up to a factor of 12), because the maximum variation in sample weight was of a factor of three.

Furthermore, molar extinction coefficients show a much lower distribution between them after grinding. Probably grinding of samples leads to smaller particles and smaller distribution in particles size, because agglomerates in the sample are broken up. Hence, signal intensities of pyridine signals are higher in grounded samples which lead to larger molar extinction coefficients that can be determined more reproducibly.

Brønsted sites are only detected for the majority of the samples at an adsorption temperature of 150 °C. First of all it is very interesting to note that molar extinction coefficients of Lewis sites do not change regardless if Brønsted sites are detected in the sample or not. This shows that the method presented in Chapter 3 is suitable for the calculation of molar extinction coefficients. However, molar extinction coefficients of Brønsted sites of sample M-57 are about twice as large at 150 °C as coefficients determined at 25 °C (M-57 is the only sample where Brønsted sites are observed at 25 °C). One reason may be that higher kinetic energy of hydroxyl groups and pyridine at 150 °C lead to a higher protolysis as at 25 °C and, therefore, to the observed increase in the molar extinction coefficients.

### 5.2. Comparison of concentrations of acidic sites

Concentrations of acidic sites determined by <sup>15</sup>N MAS NMR and FTIR under various conditions are shown in Fig. 4 for Lewis sites and Fig. 5 for Brønsted sites.

It has been pointed out that molar extinction coefficients in FTIR spectroscopy exhibit a broad distribution in ungrounded samples and differ even for the same sample up to a factor of 12. Surprisingly, concentrations of acidic sites are in the same order of magnitude. The reason for different distributions in concentrations and extinction coefficients in FTIR spectroscopy is that the position of the IR beam, where it penetrates the self-supporting disc, is the same in the entire experiment. The



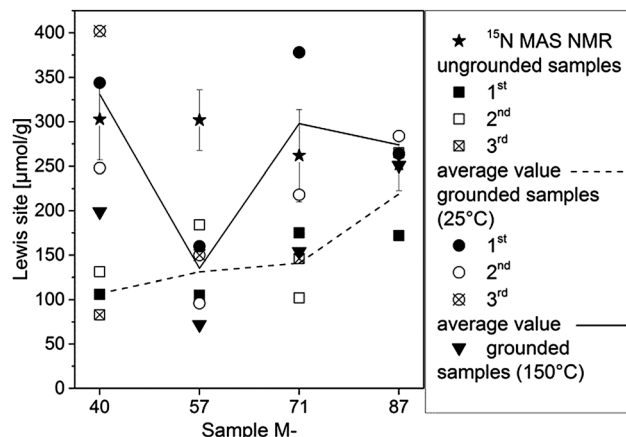


Fig. 4 Concentration of Lewis sites determined by  $^{15}\text{N}$  MAS NMR and FTIR under various conditions. Error bars shown are determined by measuring several samples (NMR). Lines indicate the average values of several FTIR measurements.

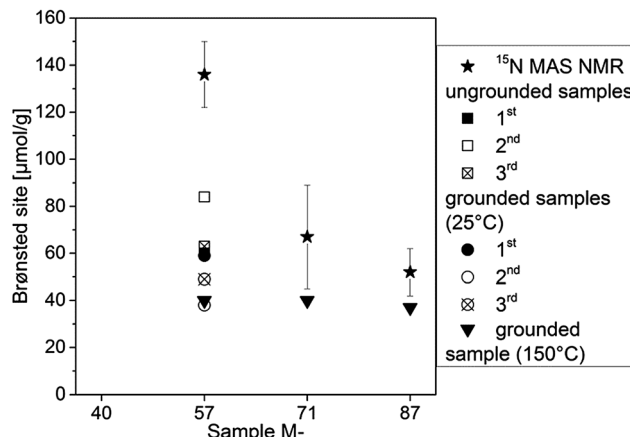


Fig. 5 Concentration of Brønsted sites determined by  $^{15}\text{N}$  MAS NMR and FTIR under various conditions. Error bars shown are determined by measuring several samples (NMR).

scattering of the IR beam and the detected signal intensities depend on the particle sizes with which the IR beam interacts.<sup>35</sup> Position of the IR beam and, thus, scattering of the IR beam is the same during the entire experiment. Therefore, the signal intensities of the pyridine signal are of the same order of magnitude during the adsorption of pyridine and after all acidic sites are saturated with pyridine. Hence, the effect of the particle sizes on the signal intensity is cancelled out in the division of the signal area by the molar extinction coefficient in the calculation of the amount of acidic sites (eqn (5)). Therefore, concentrations of acidic sites can be determined reproducibly although molar extinction coefficients differ.

Concentrations of acidic Lewis sites are larger in grounded samples in comparison to ungrounded samples. To ensure that the grinding does not create new surfaces and therefore new acidic sites, the surface area was measured by nitrogen sorption before and after grinding of one sample (see Table 1 in the ESI†). It can be seen that the surface area does not increase significantly after grinding of the sample. Hence, no new acidic sites are created due to the grinding. Nevertheless, concentrations of acidic sites determined by FTIR are affected by grinding of the samples. In two samples M-40 and M-71, three times more acidic Lewis sites are detected by FTIR after grinding. The reason may be that bigger particles/agglomerates in ungrounded samples are held together by the interaction of basic hydroxyl groups or fluoride with acidic Lewis sites. Grinding of the samples probably breaks up these agglomerates, such that these acidic Lewis sites are accessible to pyridine at 25 °C.

Furthermore, it has been seen that FTIR signals of pyridine at Brønsted sites occur in some samples only after treatment at 150 °C. Hence, FTIR experiments were performed at pyridine adsorption temperature of 150 °C. FTIR adsorption experiments at 150 °C show two differences compared to the same experiments at 25 °C. Firstly, Brønsted sites can be detected in three of the samples at 150 °C, whereas at 25 °C only M-57 shows signals for pyridine at Brønsted sites. The reason may be that Brønsted

sites are difficult to access even in grounded samples and hence the increased protolysis or pyridine mobility at 150 °C is necessary to protonate pyridine. Secondly, concentrations of acidic sites are lower in all samples at higher temperature. The reason for the lower concentrations may be the fact that during desorption (150 °C and high vacuum  $10^{-5}$  to  $10^{-6}$  mbar) of weakly adsorbed pyridine molecules pyridine also partly desorbs from the weak acidic sites of the investigated samples. Furthermore, adsorption of pyridine at an acidic site is an exothermal process and therefore less favorable at higher temperatures and weak sites. Hence, the equilibrium constants of the reactions between pyridine and the acidic Lewis and Brønsted sites may be small at 150 °C.

Comparison of quantification by NMR (sample preparation: excess of  $^{15}\text{N}$ -pyridine was added and distributed in the sample for 30 min at 150 °C. After that, the sample was evacuated ( $10^{-2}$  mbar) for 1 h at 150 °C) with the quantitative experiments by FTIR (see Fig. 4 and 5) shows that the total concentration of acidic sites cannot be measured properly with any of the used experimental conditions in the FTIR experiments (either in grounded or ungrounded samples and pyridine adsorbed *via* gas phase at 25 °C or 150 °C).

Concentrations of Lewis sites could be determined properly, for the majority of the catalysts, only in grounded samples at 25 °C by FTIR. However, under these conditions Brønsted sites were only detected in one catalyst by FTIR while NMR detect in three of the catalysts (M-57, M-71 and M-87) Brønsted sites. That in these three catalysts Brønsted sites exist is supported by FTIR experiments at 150 °C.

Moreover, the determined concentrations of acidic sites of sample M-57 by  $^{15}\text{N}$  MAS NMR are higher than in all FTIR investigations, regardless which experimental condition was used. Quantification by NMR shows that this catalyst exhibits the highest amount of acidic Brønsted sites. Maybe interaction of pyridine molecules with hydroxyl groups disturb the background signals between 1750 and 1300  $\text{cm}^{-1}$  (see Fig. 15 in ESI†), which lead to errors in the FTIR difference spectra.





## 6. Conclusion

A series of weak acidic hydroxylated magnesium fluorides was investigated by quantitative FTIR carried out under various experimental conditions and quantitative solid state  $^{15}\text{N}$  MAS NMR. Both methods use pyridine as probe molecule, so that the determined concentrations of acidic sites can be compared. For the quantification by FTIR spectroscopy, it is crucial to determine molar extinction coefficients for Lewis and Brønsted sites. An easy method was presented which allow the calculation of molar extinction coefficient from a single sample. Determination of molar extinction coefficients from a single sample is important because this investigation shows that molar extinction coefficients differ in the investigated series of samples and even between various measurements of the same sample. Hence, molar extinction coefficients determined for one sample cannot be transferred to another sample. The variance in molar extinction coefficients can be explained by different particle sizes in the samples which influence the signal intensity in the FTIR spectra. Accordingly, molar extinction coefficients can be calculated more reproducible if the samples are finely grounded to ensure a small distribution of particle sizes.

Furthermore, it was found that acidic sites are partially not accessible for pyridine adsorbed *via* gas phase at 25 °C in ungrounded samples. One reason may be that large particles/agglomerates are held together by the interaction of basic hydroxyl groups or fluoride with acidic Lewis sites. Grinding of the samples breaks up these agglomerates, such that all Lewis sites were accessible to pyridine. However, even in finely grounded samples, Brønsted sites were only detected at high adsorption temperatures of pyridine in most of the samples. The reason is that Brønsted sites are difficult to access even in grounded samples and increased protolysis and/or higher pyridine mobility at higher temperature are necessary for the protonation of pyridine.

Hence, experimental conditions have to be chosen carefully for quantitative FTIR experiments and results should be compared with other quantification methods to ensure that all acidic sites were detected.

Solid state  $^{15}\text{N}$  NMR is a much more reliable method for the quantification of acid sites as both kind of acidic sites could be reliable detected and quantified.

## References

- 1 I. Agirrezabal-Telleria, Y. Guo, F. Hemmann, P. L. Arias and E. Kemnitz, *Catal. Sci. Technol.*, 2014, **4**, 1357–1368, DOI: 10.1039/c4cy00129j.
- 2 I. Agirrezabal-Telleria, F. Hemmann, C. Jäger, P. L. Arias and E. Kemnitz, *J. Catal.*, 2013, **305**, 81–91, DOI: 10.1016/j.jcat.2013.05.005.
- 3 F. Hemmann, C. Jäger and E. Kemnitz, *RSC Adv.*, 2014, **4**, 56900–56909, DOI: 10.1039/c4ra09477h.
- 4 E. Kemnitz and D.-H. Menz, *Prog. Solid State Chem.*, 1998, **26**, 97–153, DOI: 10.1016/S0079-6786(98)00003-X.
- 5 R. J. Gorte, *Catal. Lett.*, 1999, **62**, 1–13, DOI: 10.1023/A:1019010013989.
- 6 W. E. Farneth and R. J. Gorte, *Chem. Rev.*, 1995, **95**, 615–635, DOI: 10.1021/cr00035a007.
- 7 M. Niwa and N. Katada, *Chem. Rec.*, 2013, **13**, 432–455, DOI: 10.1002/tcr.201300009.
- 8 E. Brunner and H. Pfeifer, *NMR Spectroscopic Techniques for Determining Acidity and Basicity Acidity and Basicity*, Springer, Berlin, Heidelberg, 2008, vol. 6, DOI: 10.1007/3829\_2007\_016.
- 9 Y. Jiang, J. Huang, W. Dai and M. Hunger, *Solid State Nucl. Magn. Reson.*, 2011, **39**, 116–141, DOI: 10.1016/j.ssnmr.2011.03.007.
- 10 A. Auroux, *Top. Catal.*, 2002, **19**, 205–213, DOI: 10.1023/A:1015367708955.
- 11 A. Platon and W. J. Thomson, *Ind. Eng. Chem. Res.*, 2003, **42**, 5988–5992, DOI: 10.1021/ie030343g.
- 12 C. A. Emeis, *J. Catal.*, 1993, **141**, 347–354, DOI: 10.1006/jcat.1993.1145.
- 13 I. S. Pieta, M. Ishaq, R. P. K. Wells and J. A. Anderson, *Appl. Catal., A*, 2010, **390**, 127–134, DOI: 10.1016/j.apcata.2010.10.001.
- 14 E. Selli and L. Forni, *Microporous Mesoporous Mater.*, 1999, **31**, 129–140, DOI: 10.1016/S1387-1811(99)00063-3.
- 15 A. Vimont, J. C. Lavalley, L. Francke, A. Demourgues, A. Tressaud and M. Daturi, *J. Phys. Chem. B*, 2004, **108**, 3246–3255, DOI: 10.1021/jp036496z.
- 16 D. J. Rosenberg, B. Bachiller-Baeza, T. J. Dines and J. A. Anderson, *J. Phys. Chem. B*, 2003, **107**, 6526–6534, DOI: 10.1021/jp034190m.
- 17 D. J. Rosenberg and J. A. Anderson, *Catal. Lett.*, 2004, **94**, 109–113, DOI: 10.1023/B:CATL.0000019339.91894.6e.
- 18 F. Thibault-Starzyk, B. Gil, S. Aiello, T. Chevreau and J. P. Gilson, *Microporous Mesoporous Mater.*, 2003, **67**, 107–112, DOI: 10.1016/j.micromeso.2003.10.016.
- 19 F. Hemmann, I. Agirrezabal-Telleria, E. Kemnitz and C. Jäger, *J. Phys. Chem. C*, 2013, **117**, 14710–14716, DOI: 10.1021/jp405213x.
- 20 F. Hemmann, G. Scholz, K. Scheurell, E. Kemnitz and C. Jäger, *J. Phys. Chem. C*, 2012, **116**, 10580–10585, DOI: 10.1021/jp212045w.
- 21 D. Dambournet, H. Leclerc, A. Vimont, J. C. Lavalley, M. Nickkho-Amiry, M. Daturi and J. M. Winfiel, *Phys. Chem. Chem. Phys.*, 2009, **11**, 1369–1379, DOI: 10.1039/b811691a.
- 22 C. Morterra, G. Cerrato, P. Cuzzato, A. Masiero and M. Padovan, *J. Chem. Soc., Faraday Trans.*, 1992, **88**, 2239–2250, DOI: 10.1039/ft9928802239.
- 23 C. Morterra, G. Magnacca and V. Bolis, *Catal. Today*, 2001, **70**, 43–58, DOI: 10.1016/S0920-5861(01)00406-0.
- 24 S. Wuttke, S. M. Coman, G. Scholz, H. Kirmse, A. Vimont, M. Daturi, S. Schroeder and E. Kemnitz, *Chem.-Eur. J.*, 2008, **14**, 11488–11499, DOI: 10.1002/chem.200801702.
- 25 E. Kemnitz, S. Wuttke and S. M. Coman, *Eur. J. Inorg. Chem.*, 2011, **2011**, 4773–4794, DOI: 10.1002/ejic.201100539.
- 26 S. Wuttke, A. Vimont, L.-C. Lavalley, M. Daturi and E. Kemnitz, *J. Phys. Chem. C*, 2010, **114**, 5113–5120, DOI: 10.1021/jp911584h.



- 27 A. E. Bennett, C. M. Rienstra, M. Auger, K. V. Lakshmi and R. G. Griffin, *J. Chem. Phys.*, 1995, **103**, 6951–6958, DOI: 10.1063/1.470372.
- 28 D. Massiot, F. Fayon, M. Capron, I. King, S. Le Calve, B. Alonso, J.-O. Durand, B. Bujoli, Z. Gan and G. Hoatson, *Magn. Reson. Chem.*, 2002, **40**, 70–76, DOI: 10.1002/mrc.984.
- 29 C. Jaeger and F. Hemmann, *Solid State Nucl. Magn. Reson.*, 2013, **57–58**, 22–28, DOI: 10.1016/j.ssnmr.2013.11.002.
- 30 D. M. Grant and R. K. Harris, *Encyclopedia of Nuclear Magnetic Resonance*, John Wiley & Sons Ltd., Chichester, U.K., 1996, vol. 5, p. 3247.
- 31 D. A. Torchia, *J. Magn. Reson.*, 1978, **30**, 613–616, DOI: 10.1016/0022-2364(78)90288-3.
- 32 A. A. Gurinov, Y. A. Rozhkova, A. T. Zuka, J. I. Cejka and I. G. Shenderovich, *Langmuir*, 2011, **27**, 12115–12123, DOI: 10.1021/la2017566.
- 33 M. S. Solum, K. L. Altmann, M. Strohmeier, D. A. Berges, Y. Zhang, J. C. Facelli, R. J. Pugmire and D. M. Grant, *J. Am. Chem. Soc.*, 1997, **119**, 9804–9809, DOI: 10.1021/ja964135+.
- 34 J. Noack, K. Scheurell, E. Kemnitz, P. Garcia-Juan, H. Rau, M. Lacroix, J. Eicher, B. Lintner, T. Sontheimer, T. Hofmann, J. Hegmann, R. Jahn and P. Löbmann, *J. Mater. Chem.*, 2012, **22**, 18535–18541, DOI: 10.1039/c2jm33324d.
- 35 J. M. Chalmers, Mid-Infrared Spectroscopy: Anomalies, Artifacts and Common Errors, in *Handbook of Vibrational Spectroscopy*, 2006, DOI: 10.1002/0470027320.s3101.
- 36 F. C. Jentoft, J. Kröhnert, I. R. Subbotina and V. B. Kazansky, *J. Phys. Chem. C*, 2013, **117**, 5873–5881, DOI: 10.1021/jp4004856.

